



## Impact of Outer Fuel Cycle Tritium Transport on Initial Start-Up Inventory for Next Fusion Devices

Marco Riva, Alice Ying, Mohamed Abdou, Mu-Young Ahn & Seungyon Cho

To cite this article: Marco Riva, Alice Ying, Mohamed Abdou, Mu-Young Ahn & Seungyon Cho (2019): Impact of Outer Fuel Cycle Tritium Transport on Initial Start-Up Inventory for Next Fusion Devices, Fusion Science and Technology, DOI: [10.1080/15361055.2019.1643691](https://doi.org/10.1080/15361055.2019.1643691)

To link to this article: <https://doi.org/10.1080/15361055.2019.1643691>



Published online: 06 Aug 2019.



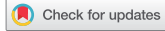
Submit your article to this journal [↗](#)



Article views: 14



View Crossmark data [↗](#)



# Impact of Outer Fuel Cycle Tritium Transport on Initial Start-Up Inventory for Next Fusion Devices

Marco Riva,<sup>a\*</sup> Alice Ying,<sup>a</sup> Mohamed Abdou,<sup>a</sup> Mu-Young Ahn,<sup>b</sup> and Seungyon Cho<sup>b</sup>

<sup>a</sup>University of California, Los Angeles, Mechanical and Aerospace Engineering Department, Los Angeles, California

<sup>b</sup>National Fusion Research Institute, Daejeon, Korea

Received June 14, 2018

Accepted for Publication July 11, 2019

**Abstract** — In this paper, dynamic tritium flow rates and inventories of the outer fuel cycle (OFC) of a DEMONstration nuclear fusion reactor (DEMO) are analyzed to determine the initial amount of tritium that has to be prepared to sustain plasma operation at reactor start-up, i.e., until tritium bred in blankets is extracted and available. The main components of the helium coolant ceramic reflector tritium breeding system were modeled in detail with the use of COMSOL Multiphysics and integrated into a system-level model within the MATLAB/Simulink platform to simulate OFC tritium streams. Furthermore, a control volume analysis was derived to incorporate the OFC flow rates calculated with the dynamic integrated numerical tool for initial start-up tritium inventory (ISTI) analysis. We found that the tritium processing time of the tritium extraction system (TES) plays a critical role for ISTI assessment. On one hand, for batchwise technology such as adsorption/regeneration columns, the OFC-attributed ISTI is ~2.6 kg calculated for a 3-GW fusion power reactor. On the other hand, online extraction techniques such as catalytic membrane reactors offer continuous operation and result in ~10 to 250 g of ISTI depending on the TES efficiency and breeder material tritium residence time. The helium coolant system (HCS) line has a minor impact on ISTI since tritium retention in HCS components is orders of magnitude lower than the TES line when a tungsten plasma-facing-component coating is implemented.

**Keywords** — Initial start-up tritium inventory, outer fuel cycle, tritium extraction system, time-dependent tritium inventories.

**Note** — Some figures may be in color only in the electronic version.

## I. INTRODUCTION

Accurate estimation of time-dependent tritium inventories and flow rates in fusion reactor components is critical to meet nuclear licensing criteria and safety regulations. Moreover, reserves of natural tritium are very limited, and the fuel is very precious. For tritium economy and fusion commercialization, a balanced budget is critical.

A great deal of work on tritium fuel cycle dynamic modeling is reported in the literature. Most studies are

based on the residence time approach, i.e., the average time tritium stays in a component before it is released. In these studies, the overall fusion fuel cycle is modeled by systems of time-dependent zero-dimensional (0-D) ordinary differential equations describing tritium flow rates.<sup>1-4</sup> Kuan and Abdou proposed a new modeling approach by introducing more physics for each fuel cycle component and accounting for more realistic operation parameters.<sup>5</sup> However, because of the lack of detailed reactor design and limited computational capabilities, the model still used a 0-D description for fusion subsystems. With the development of finite element solvers, several research groups started to model fusion fuel cycle detailed components,<sup>6-9</sup> i.e., considering two-dimensional

---

\*E-mail: [marco@fusion.ucla.edu](mailto:marco@fusion.ucla.edu)

/three-dimensional complex geometries and solving constitutive equations. Recently, an effort was launched to incorporate high-resolution detailed models to system level to reproduce the fuel cycle dynamic. A dynamic tritium transport model,<sup>10</sup> where detailed components modeled with COMSOL Multiphysics<sup>11</sup> are integrated to system level through the MATLAB/Simulink computational platform,<sup>12</sup> was presented for the helium coolant ceramic reflector tritium breeding system.

Analysis and assessment of tritium inventories and flow rates through system-level models can be extended to determining key parameters impacting fusion technology feasibility and economy such as the initial start-up tritium inventory (ISTI) and the tritium breeding ratio (TBR) that is required TBR<sub>r</sub>, as seen in Refs. 1 through 5. The fuel cycle comprehends several subsystems characterized by different functions, requirements, conditions, and physics. We can divide the overall fuel cycle into (1) inner fuel cycle (IFC), i.e., plasma exhaust, fuel cleanup, isotope separation, and delivery systems, and (2) outer fuel cycle (OFC), i.e., first wall (FW)/divertor, blanket, coolant, and purge gas processing systems. Current experimental fusion reactors are characterized by relatively low fueling efficiency (<50%) and tritium fractional burnup [~0.35% calculated for ITER (Ref. 13)]. Therefore, a large part of tritium contained in the vacuum vessel is exhausted through the pumping duct to the processing line of the IFC. In particular, ISTI is driven by the tritium fractional burnup  $f_b$ , fueling efficiency  $\eta_f$ , and processing time  $t_p$  of the tritium recovery systems: for  $f_b \times \eta_f < 2\%$  and  $t_p > 6\text{h}$ ,  $\text{ISTI} > 10\text{kg}$  is the consequence of the other two parameters  $f_b \times \eta_f$  and  $t_p$  (Ref. 4). In this case the IFC is dominant since most inventories are found within the IFC. However, the IFC impact on ISTI can be reduced if the product  $f_b \times \eta_f$  increases to values higher than 2% and the processing times of the IFC components are reduced, as seen in Ref. 4. Recently, Day and Giegerich proposed the so-called direct internal recycling (DIR) concept,<sup>14</sup> which aims to recycle tritium exhausted through the pumping duct directly to the plasma, to further minimize tritium retention in the IFC compartments, and found that the IFC inventory drops to ~1 kg (see Ref. 15). In all these cases ( $f_b \times \eta_f > 2\%$  or minimum processing times/DIR), the OFC becomes dominant for ISTI assessment since most tritium inventory resides in the OFC.

In detail, this paper aims to evaluate the OFC impact on ISTI. The analysis is performed to assess the effect of (1) ceramic breeder tritium residence time  $\tau_{res}$ , e.g., extrusion-spheronization sintering processed  $\text{Li}_2\text{TiO}_3$  and melt spray  $\text{Li}_4\text{SiO}_4$ —these are examples of breeders with a distinct

difference in residence time due to a different fabrication technique; (2) tritium processing time of tritium extraction systems (TESs)  $\tau_p$ , e.g., online (continuous) technology such as membrane reactors and PERMCAT (Ref. 16) and batchwise mode of adsorption/regeneration columns<sup>17</sup>; and (3) material choices of plasma-facing components (PFCs), e.g., pure advanced reduced activation alloy (ARAA) and ARAA with tungsten coating (2-mm thickness). We define the OFC-attributed ISTI as the initial amount of tritium that we need to prepare to run the reactor in question until tritium produced in its blankets is recovered and available online (assessment of tritium accumulation to start-up following reactors and TBR<sub>r</sub> assessment are beyond the scope of this research).

A mathematical formulation for OFC-attributed ISTI is derived through control volume analysis on tritium flow rates incorporating the OFC in Sec. II.A. Such flow rates are computed with an updated version of the tritium transport integrated dynamic model presented in Ref. 10 as described in Sec. II.B. With this innovative approach, it is possible to evaluate ISTI for specific fuel cycle designs under a prototypical fusion environment, which never was addressed with previous 0-D lumped models.

## II. DEFINITION OF THE PROBLEM

### II.A. IFC and OFC Contributions to ISTI

The OFC includes two main processing lines: the TES and the helium coolant system (HCS). On one hand, the HCS main goal is to maintain the OFC within the nominal temperature range by extracting heat generated in PFCs/blanket systems. Because of charge exchange neutrals (CXNs) and ion fluxes at the PFC surface, tritium implantation into the PFCs and permeation to the coolant occur. The tritium content in the coolant gas is controlled with the coolant purification system (CPS). Therefore, the ISTI must account for the inventories of the HCS/CPS components. Tritium produced in breeding blankets needs to be extracted from its carrier, e.g., helium purge gas for ceramic breeder concepts, before it reaches the IFC where it will be further processed, e.g., in the fuel cleanup and isotope separation units. This operation is performed by the TES, which should be designed to operate quickly and reduce possible delays between tritium production and extraction. Therefore, the ISTI problem for the TES line results in the determination of the effective tritium extraction time  $\tau_{eff}^{TES}$ , which we define as the time needed for the tritium

flow rates extracted from the TES,  $\dot{m}_{out}^{TES}$ , to match the value of the tritium burning rate in plasma  $\dot{N}^-$ , i.e.,  $\tau_{eff}^{TES} = t|\dot{m}_{out}^{TES} = \dot{N}^-$ .

A schematic of a typical OFC scheme, representing the main components and tritium flow rates, is presented in Fig. 1 while the variables of interest are listed in Table I.

To quantify the OFC impact on ISTI, a control volume analysis for the system of Fig. 1 is proposed. The rate of inventory change in the OFC is

$$\begin{aligned} \frac{dI_{OFC}}{dt} = & \dot{N}^+ + \Phi_{FW}^{CXN} A_{FW} + \Phi_{Div}^{CXN} A_{Div} - J_{perm}^{TES} \\ & - \dot{m}_{out}^{TES} - r_{FW} \Phi_{FW}^{CXN} A_{FW} - r_{Div} \Phi_{Div}^{CXN} A_{Div} \\ & - J_{FW,r}^{CXN} - J_{Div,r}^{CXN} - J_{perm}^{SG} - J_{perm}^{HCS} - \dot{m}_{out}^{CPS}, \end{aligned} \quad (1)$$

where  $A_{FW}$  and  $A_{Div}$  are the surface areas of the FW and divertor. The total amount of tritium inventory buildup in the OFC, i.e., the TES and HCS lines, can be found by integrating Eq. (1) in time. By summing and subtracting  $\dot{m}_{BZ,HCS}$  to the right side of Eq. (1), we can separate the contributions of the TES  $I_{OFC}^{TES}$  line and the HCS  $I_{OFC}^{HCS}$  line as follows:

$$\frac{dI_{OFC}^{TES}}{dt} = \dot{N}^+ - \dot{m}_{out}^{TES} - J_{perm}^{TES} - \dot{m}_{BZ,HCS} \quad (2)$$

and

$$\begin{aligned} \frac{dI_{OFC}^{HCS}}{dt} = & \Phi_{FW}^{CXN} A_{FW} (1 - r_{FW}) + \Phi_{Div}^{CXN} A_{Div} (1 - r_{Div}) \\ & + \dot{m}_{BZ,HCS} - J_{FW,r}^{CXN} - J_{Div,r}^{CXN} - J_{perm}^{SG} \\ & - J_{perm}^{HCS} - \dot{m}_{out}^{CPS}. \end{aligned} \quad (3)$$

Noting that  $\dot{N}^+ = TBR \times \dot{N}^- = \dot{N}^- + (TBR - 1)\dot{N}^-$ , integrating Eq. (2) with respect to time and rearranging, we obtain

$$\begin{aligned} I_{OFC}^{TES}(t) = & \int_0^t (\dot{N}^- - \dot{m}_{out}^{TES}) d\tilde{t} + \int_0^t (TBR - 1)\dot{N}^- d\tilde{t} \\ & - \int_0^t (J_{perm}^{TES} + \dot{m}_{BZ,HCS}) d\tilde{t}. \end{aligned} \quad (4)$$

The first term on the right side of Eq. (4) represents the difference between the amount of tritium burned in the plasma and extracted from the TES. This can be further split in the intervals  $[0, \tau_{eff}^{TES}]$ , where  $\dot{N}^- > \dot{m}_{out}^{TES}$ , and tritium must be supplied to the reactor from an external source, i.e., during TES processing when bred tritium is not available, and  $[\tau_{eff}^{TES}, t]$ , for which  $\dot{m}_{out}^{TES} > \dot{N}^-$  and tritium accumulation can begin. Therefore, Eq. (4) is rewritten as

$$\begin{aligned} I_{OFC}^{TES}(t) = & \int_0^{\tau_{eff}^{TES}} (\dot{N}^- - \dot{m}_{out}^{TES}) d\tilde{t} + \int_{\tau_{eff}^{TES}}^t (\dot{N}^- - \dot{m}_{out}^{TES}) d\tilde{t} \\ & + \int_0^t (TBR - 1)\dot{N}^- d\tilde{t} - \int_0^t (J_{perm}^{TES} + \dot{m}_{BZ,HCS}) d\tilde{t}. \end{aligned} \quad (5)$$

Considering the right side of Eq. (5), we define the first term as the OFC TES-attributed ISTI; the second term (negative in the balance) represents the amount of tritium that is extracted from the TES as the net of the tritium burning rate in plasma, i.e., the tritium that can be accumulated to generate the fuel reserve and start-up inventory for other reactors; the third term is the extra amount of tritium produced due to the TBR margin, i.e.,  $\dot{N}^+ - \dot{N}^-$ ; and finally, the last term represents the tritium lost via permeation to the coolant line and buildings. Note that tritium losses due to permeation from the TES line to buildings are not included in the ISTI definition. In fact, the TES line processes tritium that is bred in the blanket breeding zones

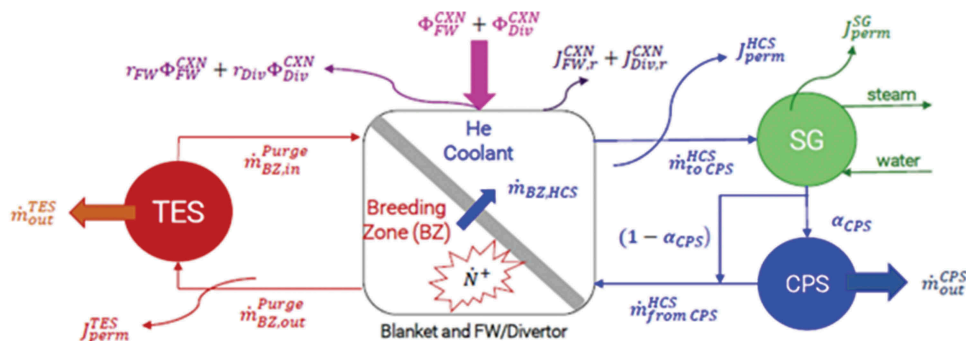


Fig. 1. Schematic of OFC main components and tritium flow rates.

TABLE I

List of Variables Used to Describe OFC Tritium Flow Rates

Variable	Description
$\dot{N}^+$ (kg/s)	Tritium production rate
$\dot{m}_{BZ,out}^{Purge}$ (kg/s)	Purge gas flow rate BZ outlet
$\dot{m}_{BZ,in}^{Purge}$ (kg/s)	Purge gas flow rate BZ inlet
$\dot{m}_{out}^{TES}$ (kg/s)	Tritium flow rate extracted from TES
$J_{perm}^{TES}$ (kg/s)	TES tritium losses to building via permeation
$\dot{m}_{BZ,HCS}$ (kg/s)	Tritium flow rate permeated to coolant from BZ
$\Phi_{FW}^{CXN}$ (kg/m <sup>2</sup> -s)	CXN flux to FW
$\Phi_{Div}^{CXN}$ (kg/m <sup>2</sup> -s)	CXN flux to divertor
$r_{FW}$	FW reflection coefficient
$r_{Div}$	Divertor reflection coefficient
$J_{FW,r}^{CXN}$ (kg/s)	FW CXN reemission to plasma flux
$J_{Div,r}^{CXN}$ (kg/s)	Divertor CXN reemission to plasma flux
$\dot{m}_{toCPS}^{HCS}$ (kg/s)	Tritium flow rate in coolant to CPS
$\dot{m}_{fromCPS}^{HCS}$ (kg/s)	Tritium flow rate in coolant from CPS
$\alpha_{CPS}$	Fraction of total coolant flow rate treated in CPS
$\dot{m}_{out}^{CPS}$ (kg/s)	Tritium flow rate extracted from CPS
$J_{perm}^{HCS}$ (kg/s)	HCS tritium losses to building via permeation
$J_{perm}^{SG}$ (kg/s)	HCS tritium losses to steam generator via permeation

(BZs) and, thus, not initially part of the start-up inventory. To conclude, the OFC TES-attributed ISTI is

$$ISTI_{OFC}^{TES} = \int_0^{\tau_{eff}^{TES}} (\dot{N}^+ - \dot{m}_{out}^{TES}) d\tilde{t}. \quad (6)$$

The OFC HCS total inventory is given by integrating Eq. (3) with respect to time:

$$J_{OFC}^{HCS}(t) = \int_0^t \{ \Phi_{FW}^{CXN} A_{FW} (1 - r_{FW}) + \Phi_{Div}^{CXN} A_{Div} (1 - r_{Div}) + \dot{m}_{BZ,HCS} - J_{FW,r}^{CXN} - J_{Div,r}^{CXN} - J_{perm}^{SG} - J_{perm}^{HCS} - \dot{m}_{out}^{CPS} \} d\tilde{t}. \quad (7)$$

The initial start-up inventory for the OFC HCS line  $ISTI_{OFC}^{HCS}$  should include the component inventory [Eq. (7)] and tritium losses due to permeation to the building, i.e.,  $J_{perm}^{SG}$  and  $J_{perm}^{HCS}$ , since both contributions are tritium sinks subtracting fuel to the plasma, evaluated in the short term, i.e., for  $t = \tau_{eff}^{TES}$ . In fact, for  $t > \tau_{eff}^{TES}$ , tritium produced in the blanket

modules is recovered, and the TBR margin compensates for losses. Furthermore, the term  $\dot{m}_{BZ,HCS}$  should not be included in  $ISTI_{OFC}^{HCS}$  since this is tritium coming from the TES line and not from plasma. Hence,

$$ISTI_{OFC}^{HCS} = I_{OFC}^{HCS} \left( t = \tau_{eff}^{TES} \right) + \int_0^{\tau_{eff}^{TES}} (J_{perm}^{SG} + J_{perm}^{HCS} - \dot{m}_{BZ,HCS}) d\tilde{t}. \quad (8)$$

Moreover, to be conservative, we also neglect tritium recovered from the CPS, which is expected to process very small fractions of the total coolant flow rate, e.g.,  $\alpha_{CPS} = 0.1\%$  to  $1\%$ , and longer times could be required. Therefore,

$$ISTI_{OFC}^{HCS} \approx \int_0^{\tau_{eff}^{TES}} \{ \Phi_{FW}^{CXN} A_{FW} (1 - r_{FW}) + \Phi_{Div}^{CXN} A_{Div} (1 - r_{Div}) - J_{FW,r}^{CXN} - J_{Div,r}^{CXN} \} d\tilde{t}. \quad (9)$$

Equation (9) corresponds to the total amount of tritium implanted into PFCs that will generate inventory in PFCs  $I_{PFC}$  and thus permeation to coolant  $J_{PFC}^{Coolant}$ .

Finally, the OFC-attributed ISTI,  $ISTI_{OFC}$ , is the sum of contributions from the TES [Eq. (6)] and the HCS ([Eq. (9)]:  $ISTI_{OFC} \approx ISTI_{OFC}^{TES} + ISTI_{OFC}^{HCS}$ .

## II.B. Computational Model

The computational model used in this analysis is an updated version of the dynamic COMSOL–MATLAB/Simulink for OFC tritium transport presented in Ref. 10. The model comprises (1) the TES line, i.e., the BZ, extraction systems, heat exchanger, H<sub>2</sub> makeup units, and connecting pipes (DN15/40S), and (2) the HCS line, i.e., the FW/divertor, CPS, and connecting pipes (DN80/80S). The physics implemented in the model includes tritium mass transport, isotope swamping effect, chemical reactions, heat transfer, and compressible purge gas flow through porous media. Details of the mathematical formulation are available in Refs. 6, 7, 8, and 18. The Simulink setup and COMSOL convergence were optimized to allow higher computational performance; the computational time was reduced by one-half compared to the model presented in Ref. 10.

For TES modeling, an analytical formulation is adopted for the online (continuous operation) case; particularly, the TES is characterized by extraction efficiency  $\eta_{TES}$ , and  $\dot{m}_{out}^{TES} = \eta_{TES} \dot{m}_{in}^{TES}$ . In the case of batchwise

operation, detailed modeling of the cryogenic molecular sieve bed (CMSB) was performed; the constitutive equations implemented are presented in Ref. 19. The sieve bed adopted is Zeolite 5A, the particle diameter is  $2.0 \times 10^{-3}$ , the packing of the bed is 58%, the column height is 0.86 m, and the internal diameter is 0.31 m. Adsorption is performed at 77 K while regeneration is at 100 K to enhance tritium release and reduce the processing time of the regeneration phase. Note that the CMSB treats only molecular hydrogen isotopes, i.e.,  $H_2$  and HT, while the oxidized molecules, i.e., HTO, are treated in a different unit, e.g., the room temperature molecular sieve followed by the water detritiation process. However, for the helium-cooled ceramic reflector HCCR blanket, HT represents >95% of the tritium content in purge gas at the BZ outlet, which controls the availability of bred tritium for use in fueling.

Note that the  $ISTI_{OFC}$  problem incorporates short-term inventories, i.e., inventories characteristic of the system at a time equal to  $\tau_{eff}^{TES}$ , which falls within the range of 1 h to 5 days depending on technology used for tritium extraction. For this timescale, i.e., reactor beginning of life, the reactor is subject to low irradiation dose (<0.3 displacements per atom); therefore, tritium retention due to ion- and neutron-induced trapping does not have a significant effect on start-up problems (while it affects long-term tritium retention). Moreover, because of the low trapping energies, i.e., 0.85 eV (Ref. 20), tritium retained in intrinsic traps is detrapped at typical PFC temperatures<sup>8</sup> and is not influent for ISTI characterization. For these reasons, inventory buildup in PFCs due to trapping is insignificant and not calculated in this study. Similarly, radioactive decay losses are negligible on ISTI timescales and are not accounted for in the proposed calculation.

### III. INITIAL START-UP TRITIUM INVENTORY ASSESSMENT AND DISCUSSION

#### III.A. TES Line

Tritium flow rates recovered by TES line  $\dot{m}_{out}^{TES}$  were evaluated for tritium residence times of  $Li_4SiO_4$  and  $Li_2TiO_3$  (correlations given in Ref. 21). The OFC TES line-attributed ISTI results are extrapolated to typical DEMOnstration nuclear fusion reactor (DEMO) or future commercial reactor power of 3  $GW_{fus}$ , i.e.,  $\dot{N}^- \sim 0.459$  kg/day, and different TBR values, i.e., 1.05 to 1.20. As an example, Fig. 2 shows the flow rates at the

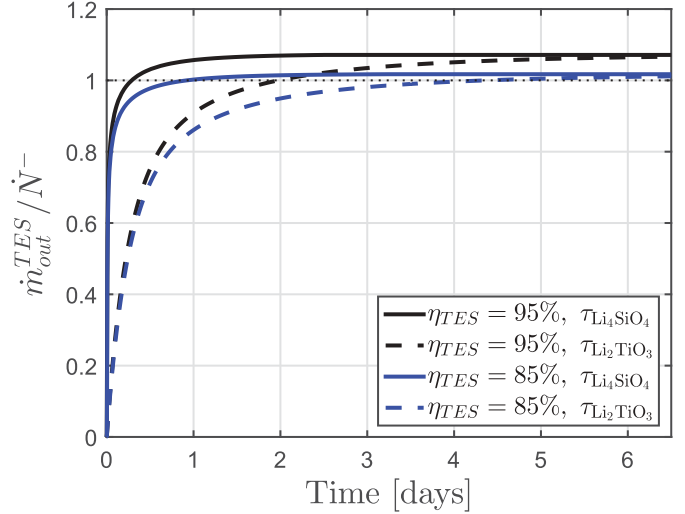


Fig. 2. Normalized tritium flow rates at TES outlet for online mode and TBR = 1.10.

TES outlet normalized by  $\dot{N}^-$  for the online (continuous) TES mode, TBR = 1.10, and TES efficiencies of 85% and 95%, and Fig. 3 shows the respective OFC TES-attributed ISTI, calculated with Eq. (6).

We found that  $\tau_{eff}^{TES}$  is less than  $\sim 0.5$  day for lithium orthosilicate while  $\sim 2$  days is required for lithium metatitanate when the efficiency is 95%. For lower TES efficiency, 85%, longer times are required, i.e.,  $\sim 1$  day for  $Li_4SiO_4$  and  $\sim 4.5$  days for  $Li_2TiO_3$ . Note that in this case  $\tau_{eff}^{TES} \sim \tau_{res}$  since  $\tau_p \sim 0$ . A longer residence time ( $Li_2TiO_3$ ) increases the OFC TES-attributed ISTI one order of magnitude ( $0.10$  kg < ISTI <  $0.25$  kg) compared to a shorter

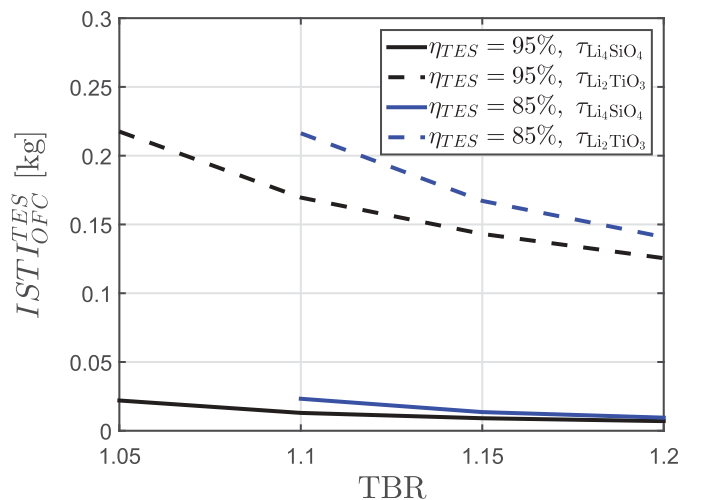


Fig. 3. The OFC TES-attributed ISTI for TES online mode.

( $\text{Li}_4\text{SiO}_4$ ) residence time ( $0.01 \text{ kg} < \text{ISTI} < 0.025 \text{ kg}$ ) while TES efficiency reduction from 95% to 85% is less impactful. However, results suggest that if the TES efficiency falls below 90% and the TBR is  $\sim 1.05$ , the tritium extracted from the TES is slightly smaller than the tritium burning rate in the plasma. Hence, further extraction must be performed downstream the TES at very low partial pressure to ensure breakeven between tritium extraction and consumption in the plasma.

In the case of batchwise operation, the total processing time of adsorption/regeneration columns can be calculated as  $\tau_p = \tau_{ad} + \tau_{reg}$ , where  $\tau_{ad}$  is the adsorption time and  $\tau_r$  is the regeneration time. This parameter varies depending on the column capacity, dimensions, operating temperature, and TBR. In our case, for the parameters given in Sec. II.B, we found that the adsorption time calculated at column saturation, i.e., when the tritium concentrations at the CMSB outlet are equal to 0.1% of the concentration at the inlet, is  $\sim 134 \text{ h}$  ( $\sim 5.6 \text{ days}$ ) for  $\text{Li}_4\text{SiO}_4$  and  $\sim 137.2 \text{ h}$  ( $\sim 5.7 \text{ days}$ ) for  $\text{Li}_2\text{TiO}_3$  (values calculated for TBR = 1.10). The time delay between breeders is due to the different tritium residence time of tritium in ceramics. The regeneration time is  $\sim 1 \text{ day}$  when performed at 100 K; however, only  $\sim 1.5 \text{ h}$  is needed to provide flow rates that overcome the tritium burning rate in the plasma, as shown in Fig. 4. Because of the long times required to reach saturation in the column during the adsorption process, the TBR effect is less noticeable compared to the online case; e.g.,  $\text{Li}_4\text{SiO}_4$  with TBR = 1.20 (best-case scenario) gives adsorption

time 3 h smaller than  $\text{Li}_2\text{TiO}_3$  with TBR = 1.05 (worst-case scenario).

We show in Table II the  $\text{ISTI}_{\text{OFC}}^{\text{TES}}$  calculated using Eq. (6). The range is 2.55 to 2.64 kg depending on the breeding material and TBR. As observed, the adsorption time is dominant in defining the effective extraction time, i.e.,  $\tau_{\text{eff}}^{\text{TES}} \sim \tau_{ad}$ , attenuating the effect of breeder choice and TBR, which accounts for  $\sim 90\%$  difference inventory.

### III.B. HCS Line

The tritium inventory buildup in the HCS components and permeation to the coolant depend on CXN implantation into the PFCs. In general, the CXN magnitude varies depending on several parameters, e.g., physics regime, scrape-off layer, and edge fueling. The presented results are obtained for the CXN tritium flux at the FW calculated for the ITER HCCR test blanket module port,<sup>22</sup> i.e.,  $10^{21} \text{ atoms/m}^2\text{-s}$  (50% D–50% T) at an energy of 400 eV. This choice is considered representative of the average implantation into the PFCs in the absence of data for the specific DEMO design. We considered different PFC structural materials: (1) pure ARAA and (2) ARAA with a tungsten coating layer (2-mm thickness). The CXN implantation spatial distribution profile in ARAA and W are derived with the SRIM/TRIM code. The reflection coefficients of ARAA and W are  $\sim 0.3$  and  $\sim 0.45$ , respectively. We found that tungsten coating reduces inventory buildup and permeation to the coolant about one to two orders of magnitude compared with the case of pure ARAA as seen in Figs. 5 and 6.

The HCS-attributed ISTI calculated with Eq. (9) for the K-DEMO (Ref. 23) PFC design with  $\dot{N}^- \sim 0.459 \text{ kg/day}$  and using the representative  $\tau_{\text{eff}}^{\text{TES}}$  of each extraction technology, material, and TBR, is shown in Fig. 7 for online operation and in Table III for the batchwise case.

## IV. CONCLUSIONS

A control volume approach analytical method has been derived to incorporate tritium flow rates calculated from an improved dynamic integrated model for tritium ISTI analysis. ISTI was evaluated for different breeder material residence times, TES operational modes, efficiencies, and PFC surface materials. The analysis shows that the TES line is dominant in

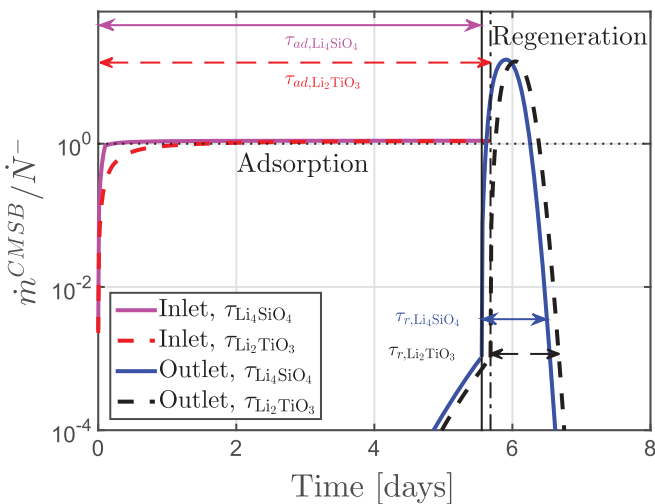


Fig. 4. The CMSB inlet/outlet flow rates for  $\text{Li}_4\text{SiO}_4$  and  $\text{Li}_2\text{TiO}_3$ .

TABLE II  
 OFC TES–Attributed ISTI for TES Operated in Batchwise Mode

$ISTI_{OFC}^{TES}$ (kg)	TBR = 1.05	TBR = 1.10	TBR = 1.15	TBR = 1.20
$Li_4SiO_4$	2.58	2.57	2.56	2.55
$Li_2TiO_3$	2.64	2.63	2.62	2.61

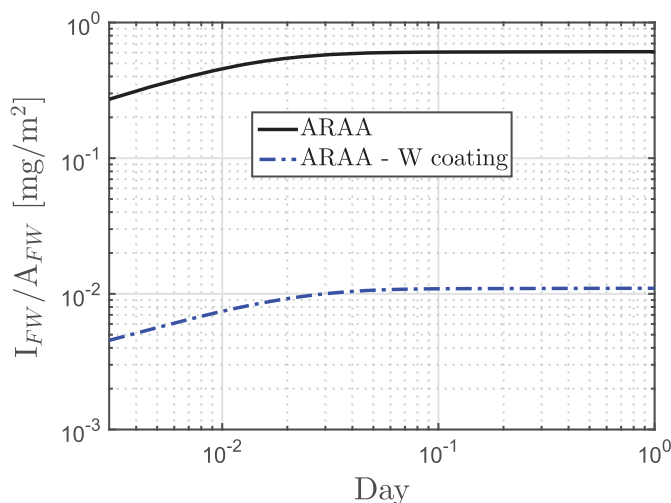


Fig. 5. Tritium inventory per unit of FW surface area.

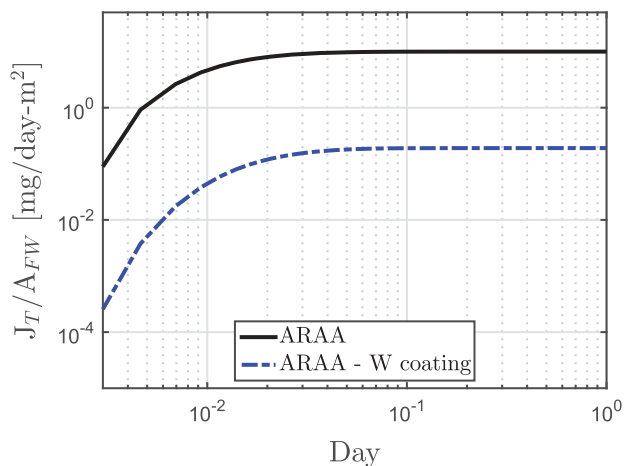
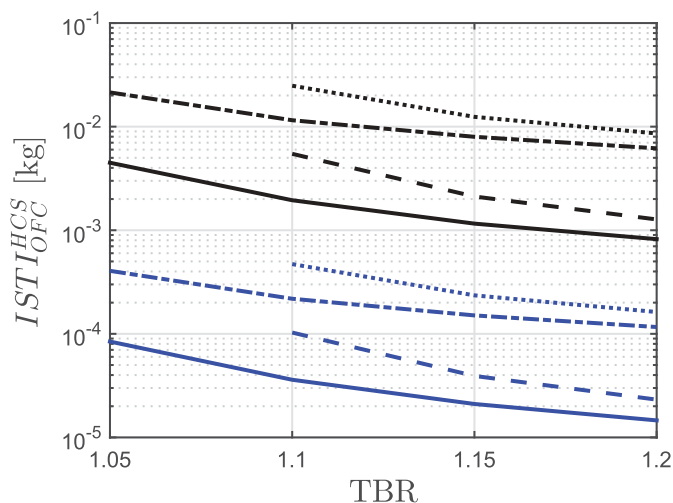


Fig. 6. Tritium permeation to coolant per unit of FW surface area.

determining the OFC impact to ISTI. The most important parameters are the residence time of tritium in the breeders and the processing time of the tritium extraction technologies that contribute to defining the effective tritium extraction time. The OFC-attributed ISTI is minimum when continuous extraction


 Fig. 7. The OFC HCS–attributed ISTI for continuous operation of TES. Black: ARAA PFCs; blue: ARAA with W coating PFCs; solid line:  $Li_4SiO_4$ ,  $\eta_{TES} = 0.95$ ; dashed line:  $Li_4SiO_4$ ,  $\eta_{TES} = 0.85$ ; dash-dot line:  $Li_2TiO_3$ ,  $\eta_{TES} = 0.95$ ; dotted line:  $Li_2TiO_3$ ,  $\eta_{TES} = 0.85$ .

technologies are implemented ( $\sim 10$  to  $250$  g) while it is considerably higher ( $\sim 2.6$  kg) when adsorption/regeneration columns are the extraction technique. In this case the processing time ( $\sim 5.5$  days) has a dominant effect over the breeder residence time (approximately hours). If the batchwise operation mode will be further developed and/or considered for future commercial reactors, research and development should focus on reducing the adsorption time and therefore the total processing time to a minimum. This implies finding the optimal column capacity/dimension and adsorption capability.

The HCS-attributed ISTI is less significant, particularly when W coating is implemented ( $ISTI_{OFC}^{HCS} \sim 10^{-5} - 10^{-3}$  kg). However, for nuclear regulation and safety, the integrated dynamic model developed and improved in this study provides means to predict, track, control, and minimize HCS inventories and permeation/losses to the environment.

TABLE III  
OFC HCS–Attributed ISTI for TES Operated in Batchwise Mode

$ISTI_{OFC}^{HCS}$ (kg)	TBR =1.05	TBR = 1.10	TBR = 1.15	TBR = 1.20
ARAA				
$Li_4SiO_4$	$3.21 \times 10^{-2}$	$3.20 \times 10^{-2}$	$3.19 \times 10^{-2}$	$3.17 \times 10^{-2}$
$Li_2TiO_3$	$3.29 \times 10^{-2}$	$3.27 \times 10^{-2}$	$3.26 \times 10^{-2}$	$3.25 \times 10^{-2}$
ARAA-W Coating				
$Li_4SiO_4$	$6.08 \times 10^{-4}$	$6.06 \times 10^{-4}$	$6.04 \times 10^{-4}$	$6.01 \times 10^{-4}$
$Li_2TiO_3$	$6.23 \times 10^{-4}$	$6.20 \times 10^{-4}$	$6.18 \times 10^{-4}$	$6.16 \times 10^{-4}$

## Acknowledgments

The authors would like to thank J. T. Van Lew for his insightful comments regarding this work. This work was supported jointly by U.S. Department of Energy contract DE-FG 03-ER52123 and by Task Agreement between UCLA-NFRI for Cooperation on R&D for Fusion Nuclear Science to Expedite the Realization of Magnetic Fusion Energy.

## ORCID

Marco Riva  <http://orcid.org/0000-0001-7262-0688>

## References

- M. ABDOU et al., “Deuterium-Tritium Fuel Self-Sufficiency in Fusion Reactors,” *Fusion Technol.*, **9**, 250 (1986); <https://doi.org/10.13182/FST86-A24715>.
- L. PAN, H. CHEN, and Q. ZENG, “Sensitivity Analysis of Tritium Breeding Ratio and Startup Inventory for CFETR,” *Fusion Eng. Des.*, **112**, 311 (2016); <https://doi.org/10.1016/j.fusengdes.2016.08.026>.
- H. CHEN et al., “Tritium Fuel Cycle Modeling and Tritium Breeding Analysis for CFETR,” *Fusion Eng. Des.*, **106**, 17 (2016); <https://doi.org/10.1016/j.fusengdes.2016.02.100>.
- M. ABDOU et al., “Blanket/First Wall Challenges and Required R&D on the Pathway to DEMO,” *Fusion Eng. Des.*, **100**, 2 (2015); <https://doi.org/10.1016/j.fusengdes.2015.07.021>.
- W. KUAN and M. ABDOU, “A New Approach for Assessing the Required Tritium Breeding Ratio and Startup Inventory in Future Fusion Reactors,” *Fusion Technol.*, **35**, 309 (1999); <https://doi.org/10.13182/FST99-A84>.
- A. YING et al., “Tritium Transport Evolutions in HCCR TBM Under ITER Inductive Operations,” *Fusion Sci. Technol.*, **68**, 2, 346 (2015); <https://doi.org/10.13182/FST14-908>.
- A. YING et al., “Advancement in Tritium Transport Simulations for Solid Breeding Blanket System,” *Fusion Eng. Des.*, **109–111**, Part B, 1511 (2016); <https://doi.org/10.1016/j.fusengdes.2015.11.040>.
- A. YING, H. LIU, and M. ADBOU, “Analysis of Tritium Retention and Permeation in FW/Divertor Including Geometric and Temperature Operating Features,” *Fusion Sci. Technol.*, **64**, 2, 303 (2013); <https://doi.org/10.13182/FST64-303>.
- M. ZUCCHETTI et al., “Tritium Modeling for ITER Test Blanket Module,” *Fusion Sci. Technol.*, **68**, 644 (2015); <https://doi.org/10.13182/FST14-959>.
- A. YING et al., “Breeding Blanket System Design Implications on Tritium Transport and Permeation with High Tritium Ion Implantation: A MATLAB/Simulink, COMSOL Integrated Dynamic Tritium Transport Model for HCCR TBS,” *Fusion Eng. Des.*, **136**, Part B, 1153 (2018); <https://doi.org/10.1016/j.fusengdes.2018.04.093>.
- “COMSOL Multiphysics with MATLAB v. 5.0,” COMSOL/Livelink (2015).
- “Simulink Developing S-Functions, MATLAB & SIMULINK,” MathWorks, Inc (2017).
- M. ABDOU, “Tritium Fuel Cycle, Tritium Inventories and Physics and Technology R&D Challenges for: 1) Enabling the Startup of DEMO and Future Power Plants and 2) Attaining Tritium Self-Sufficiency in Fusion Reactors,” *Proc. 13th Int. Symp. Fusion Nuclear Technology (ISFNT-13)*, Kyoto, Japan, September 25–29, 2017.
- C. DAY and T. GIEGERICH, “The Direct Internal Recycling Concept to Simplify the Fuel Cycle of a Fusion Power Plant,” *Fusion Eng. Des.*, **88**, 616 (2013); <https://doi.org/10.1016/j.fusengdes.2013.05.026>.
- C. DAY, “A Smart Architecture for the DEMO Fuel Cycle,” *Proc. 30th Symp. Fusion Technology*, Giardini-Naxos, Italy, September 16–21, 2018.
- D. DEMANGE et al., “Zeolite Membranes and Palladium Membrane Reactor for Tritium Extraction from the Breeder Blankets of ITER and DEMO,” *Fusion Eng. Des.*, **88**, 2396 (2013); <https://doi.org/10.1016/j.fusengdes.2013.05.102>.

17. M. ZUCCHETTI et al., “Tritium Control in Fusion Reactor Materials: A Model for Tritium Extracting System,” *Fusion Eng. Des.*, **98–99**, 1885 (2015); <https://doi.org/10.1016/j.fusengdes.2015.06.052>.
18. H. ZHANG et al., “Characterization of Tritium Isotopic Permeation Through ARAA in Diffusion Limited and Surface Limited Regimes,” *Fusion Sci. Technol.*, **72**, 416 (2017).
19. K. TANAKA, M. UETAKE, and M. NISHIKAWA, “Calculation of Breakthrough Curve of Multicomponent Hydrogen Isotopes Using Cryosorption Column,” *J. Nucl. Sci. Technol.*, **33**, 6, 492 (1996); <https://doi.org/10.1080/18811248.1996.9731942>.
20. O. V. OGORODNIKOVA et al., “Deuterium Retention in Tungsten in Dependence of the Surface Conditions,” *J. Nucl. Mater.*, **313–316**, 469 (2003); [https://doi.org/10.1016/S0022-3115\(02\)01375-2](https://doi.org/10.1016/S0022-3115(02)01375-2).
21. J. G. VAN DER LAAN et al., “Tritium Release Data for Ceramic Breeder Materials: Compilation of Results from EXOTIC-6, -7 and -8,” *Proc. 7th Int. Workshop Ceramic Breeder Blanket Interaction*, Petten, The Netherlands, September 14–16, 1998.
22. “Task Force - Test Program Preliminary Safety - Document - Working Meeting 25,” ITER site, June 7–9, 2017.
23. S. CHO et al., “Investigation of Technical Gaps Between DEMO Blanket and HCCR TBM,” *Fusion Eng. Des.*, **136**, Part A, 190 (2018); <https://doi.org/10.1016/j.fusengdes.2018.01.050>.